C-C chemokine receptor 5 signaling contributes to cardiac remodeling and dysfunction under pressure overload

XIAOMIN WANG[1-3*], WEI LI[3*], QIANG YUE[4], WEI DU[4], YONGMING LI[4], FU LIU[4], LIU YANG[5], LIJUAN XU[5], RUIPING ZHAO[2-4,6] and JIANG HU[3,4,6]

[1]Shanghai East Hospital, Tongji University School of Medicine, Shanghai 200120; [2]Baotou Central Hospital (The Post-doctoral Research Station of Clinic Medicine, Tongji University), Tongji University School of Medicine, Shanghai 200072; [3]Translational Medicine Center and [4]Department of Cardiology, Baotou Central Hospital, Donghe, Baotou 014040; [5]Department of Institution of Interventional and Vascular Surgery, Tongji University, Shanghai 200072; [6]Inner Mongolia Medical University, Hohhot, Inner Mongolia 010110, P.R. China

Received March 18, 2020; Accepted October 21, 2020

DOI: 10.3892/mmr.2020.11687

Abstract. Aortic stenosis (AS) leads to chronic pressure overload, cardiac remodeling and eventually heart failure. Chemokines and their receptors have been implicated in pressure overload-induced cardiac remodeling and dysfunction. In the present study, the role of C-C chemokine receptor 5 (CCR5) in pressure overload-induced cardiac remodeling and dysfunction was investigated in mice subjected to transverse aortic constriction (TAC). Cardiac levels of CCR5 and C-C motif chemokine ligands (CCLs)3, 4 and 5 were determined by western blotting and reverse transcription-quantitative PCR, respectively. Cardiac functional parameters were evaluated by echocardiographic and hemodynamic measurements. Myocardial fibrosis was assessed by Masson's trichrome staining and α-smooth muscle actin immunostaining. Myocardial hypertrophy and inflammatory cell infiltration were evaluated by hematoxylin and eosin staining. Angiotensin II (Ang II)-induced hypertrophy of H9c2 cardiomyocytes was assessed by F-actin immunostaining. ERK1/2 and P38 phosphorylation was examined by western blotting. TAC mice exhibited higher myocardial CCL3, CCL4, CCL5 and CCR5 levels compared with sham mice. Compared with sham mice, TAC mice also exhibited impaired cardiac function along with myocardial hypertrophy, fibrosis and inflammatory cell infiltration. TAC-induced cardiac remodeling and dysfunction were effectively ameliorated by administration of anti-CCR5 but not by IgG control antibody. Mechanistically, increased ERK1/2 and P38 phosphorylation was detected in TAC hearts and Ang II-stimulated H9c2 cardiomyocytes. Treatment with anti-CCR5 antibody decreased ERK1/2 and P38 phosphorylation and attenuated Ang II-induced H9c2 cell hypertrophy. CCR5 inhibition protected against pressure overload-induced cardiac abnormality. The findings of the present study indicate that ERK1/2 and P38 signaling pathways may be involved in the cardioprotective effects of CCR5 inhibition.

Correspondence to: Professor Ruiping Zhao, Department of Cardiology, Baotou Central Hospital, 61 Huancheng Road, Donghe, Baotou 014040, P.R. China
E-mail: ruipingzhao@163.com

*Contributed equally

Key words: aortic stenosis, transverse aortic constriction, cardiac dysfunction, cardiac remodeling, C-C chemokine receptor 5

Introduction

Aortic stenosis (AS) is the most common type of heart valve disease with an increasing prevalence; in 11,911 people with different age, sex and ethnic characteristics heart valve disease accounted for 5.2% of the elderly (>75 years) population (1). The narrowing of the exit of the left ventricle (LV) of the heart results in chronic LV pressure overloading (2). This sustained myocardial stress leads to pathological LV remodeling, characterized by concentric hypertrophy and interstitial and perivascular fibrosis (3), which increases the risk of heart failure and of mortality (25%) (4). The average overall survival rate in symptomatic patients with AS without aortic valve replacement is 2-3 years (5,6). Surgery to repair or replace the valve releases the biomechanical stress and improves LV function, and is recommended as the only lifesaving therapy for symptomatic patients (6). However, structural abnormalities in severe cases are only partially reversed following valve replacement (7). There is currently no preventive therapy for LV structural damage secondary to AS (2). Understanding the mechanisms involved in pressure overload-induced cardiac remodeling may enable development of novel drugs to delay the progression of structural abnormality before surgery and promote recovery following valve replacement.

Inflammation is a well-known contributing factor of atherosclerotic cardiovascular disease (8). Chemokines and their receptors regulate immune cell recruitment and activation and serve an important role in atherosclerosis (9). Evidence suggests that 'atherosclerosis-like' pathogenesis is involved in the initiation of AS (10). Chemokines and their receptors have also been implicated in the pathophysiology of LV remodeling and cardiac dysfunction caused by pressure overload (11-13).

In cardiac-specific transgenic mice, C-C chemokine receptor (CCR)9 knockout attenuates, whereas CCR9 overexpression enhances, pressure overload-induced cardiac hypertrophy (12). Serum chemokine (C-C motif) ligand (CCL) 21 levels are elevated in patients with AS and in mice exposed to LV pressure overload. Moreover, knockout of the CCL21 receptor CCR7 prevents pressure overload-induced LV wall thickening and functional impairment (13). CCR5 is involved in a number of autoimmune and inflammatory diseases, including rheumatoid arthritis and juvenile idiopathic arthritis, and potent CCR5 antagonists (e.g., Maraviroc) have been developed as potential therapeutics (14). CCR5 polymorphism has been linked to the degree of calcification of stenotic aortic valves (15). However, the role of CCR5 in cardiac remodeling and dysfunction under pressure overload is unclear.

Transverse aortic constriction (TAC) in mice is a common animal model used to study pressure overload-induced cardiac hypertrophy and dysfunction (16). In the present study, expression levels of CCR5 and its ligands were assessed in mice subjected to TAC. The effects of CCR5 inhibition on TAC-induced cardiac hypertrophy and dysfunction, as well as the molecular mechanisms involved, were also investigated.

Materials and methods

TAC. C57BL/6 mice (female; age 8-10 weeks; weight 18-25 g) were purchased from Shanghai Laboratory Animal Center (Shanghai, China). The breeding conditions were: 21±2˚C, 30-70% humidity, 12-h light/dark cycle and free access to food and water. TAC surgery was performed as described previously (17). The mice were deeply anesthetized by intraperitoneal injection of 10% chloral hydrate (300 mg/kg); mice showed no signs of peritonitis following injection of chloral hydrate. Anesthesia was indicated by decreased limb tension and slow corneal reflex. Briefly, aortic occlusion was achieved by tying a suture around the transverse aorta over a juxtaposed 27-gauge blunted needle placed between the innominate and left carotid arteries. The needle was then removed, resulting in a severely narrowed aortic lumen. Hearts were collected for analysis at specific time-points during a study period of 28 days. Sham-operated mice without TAC served as controls. Following TAC surgery, mice received once-daily intraperitoneal injection of 0.5 μg/g goat anti-mouse CCR5 antibody (1:500; cat. no. ab65850; Abcam), Rantes (CCR5 agonist 1:500; cat. no. ab189841; Abcam) or isotype IgG control antibody (1:1,000; cat. no. ab190475; Abcam). All animal studies were approved by the Medical Ethics Committee of Baotou Central Hospital (Baotou, China) and complied with the Principles of Laboratory Animal Care (National Society for Medical Research). All experiments were performed in accordance with the National Institutes of Health (NIH) guidelines (https://www.nih.gov/). Every effort was made to minimize suffering and the number of animals. A total of 177 mice were used in this experiment; experimental grouping and distribution of mice are presented in Table I. A total of two mice were anesthetized and died due to heart puncture and heavy bleeding due to surgical errors during the modeling process, which was within the acceptable limits of the ethical approval obtained for the present study. Health of the mice was monitored according to the time-points used in the experiment (immediately following and at 3, 7, 14, 21 and 28 days post-surgery). The humane endpoints were complete loss of appetite for 24 h or inability to eat and drink on their own, or, in the absence of anesthesia or sedation, depression with hypothermia (<37˚C). Euthanasia was performed via cervical dislocation after sampling mice. Complete heartbeat cessation and pupil dilation were considered to indicate death.

Echocardiographic and hemodynamic measurements. Mouse echocardiography was performed on a Vevo2100 imaging system (VisualSonics Inc.) with a 22-55 MHz probe. All mice were anaesthetized with ketamine (50 mg/kg) by intraperitoneal injection. Left ventricular end-systolic and -diastolic left dimensions (LVESD and LVEDD, respectively) were measured according the American Society of Echocardiography guidelines (18). LV end-diastolic and -systolic volumes (EDV and ESV, respectively) were calculated using the Simpson method of disks (19). Ejection fraction (EF) was determined using the formula EF (%) = (EDV-ESV)/EDVx100. LVEDD, LVESD and the maximal rates of rise and fall in LV pressure (+ and -dP/dt, respectively) were recorded as previously described (20). LV fractional shortening (FS) was calculated using the formula FS (%) = (LVEDD-LVESD)/LVEDDx100. All measurements were performed by an investigator blinded to treatment conditions.

Reverse transcription-quantitative (RT-q)PCR. Total RNA was isolated from mouse myocardial tissue using TRIzol (Invitrogen; Thermo Fisher Scientific, Inc.). First-strand complementary DNA was synthesized using the SuperScript III kit (Invitrogen; Thermo Fisher Scientific, Inc.) according to the manufacturer's instructions. CCL3, CCL4, CCL5, collagen I, matrix metalloproteinase (MMP)2 and 9, atrial and brain natriuretic peptide (ANP and BNP, respectively) and GAPDH mRNA expression levels were determined using SYBR-Green Real-Time PCR reagents (Invitrogen; Thermo Fisher Scientific, Inc.) on a MyiQ Single-Color Real-Time PCR Detection System (Bio-Rad Laboratories, Inc.). Primer sequences are listed in Table II. PCR conditions were 95˚C for 10 min followed by 40 amplification cycles of 95˚C for 10 sec and 72˚C for 30 sec. Data were normalized to GADPH. The relative mRNA expression levels were calculated using the $2^{-\Delta\Delta Cq}$ method (21) and are presented as fold-change compared with the control/sham group.

Western blot analysis. Mouse myocardial tissue or H9c2 cells were homogenized in RIPA buffer (Beyotime Institute of Biotechnology). Protein concentrations were determined using a bicinchoninic acid (BCA) protein assay kit (Beyotime Institute of Biotechnology). Samples (5 μl) were separated via 10% SDS-PAGE and transferred to nitrocellulose membranes (Pall Life Sciences). The membranes were blocked with 5% non-fat milk at room temperature for 2 h, followed by incubation with primary antibodies against CCR5 (1:500; cat. no. ab65850), phosphorylated (p)-ERK1 (T202) + ERK2 (T185) (1:1,000; ab201015), ERK1/2 (1:1,000; cat. no. ab184699), p-P38 (Y182) (1:500; cat. no. ab47363), P38 (1:1,000; cat. no. ab170099) and β-actin (1:2,000; cat. no. ab8226; all from Abcam) overnight at 4˚C. According to manufacturer's instructions, following incubation (for 2 h at room temperature)

Table I. Distribution of experimental mice (n=177).

Total	Groups	Type of experiment performed	Figure
45	Sham (n=5) 3 days after TAC (n=8) 7 days after TAC (n=8) 14 days after TAC (n=8) 21 days after TAC (n=8) 28 days after TAC (n=8)	RT-qPCR (CCL3, CCL4, CCL5); WB (CCR5)	1
25	Sham (n=5) TAC-Control (n=5) TAC-IgG (n=5) TAC-CCR5 agonist (n=5) TAC-CCR5 Ab (n=5)	RT-qPCR (atrial/brain natriuretic peptide)	2A and B
20	Sham (n=5) TAC-Control (n=8) TAC-IgG (n=8) TAC-CCR5Ab (n=8)	IHC (CCR5); hematoxylin-eosin staining	2C and D
20	Sham (n=5) TAC-Control (n=8) TAC-IgG (n=8) TAC-CCR5Ab (n=8)	Echocardiographic and hemodynamic measurements; IHC (α-SMA); Masson's staining; RT-qPCR (collagen I, MMP2, MMP9)	2E-J; 3
20	Sham (n=5) TAC-Control (n=8) TAC-IgG (n=8) TAC-CCR5Ab (n=8)	WB (p-ERK, ERK, p-p38, p38)	4A
18	Normal control (n=3) Ang II (n=3) Ang II + IgG (n=3) Ang II + CCR5 Ab (n=3) Ang II + U0126 (n=3) Ang II + SB203580 (n=3)	WB (p-ERK, ERK, p-p38, p38); immunofluorescence	4B and C
2	Modeling failure (n=2)	-	-
Total	n=177	-	-

TAC, transverse aortic constriction; RT-q, reverse transcription-quantitative; CCL, C-C motif chemokine ligand; WB, western blotting; CCR, C-C chemokine receptor 5; IHC, immunohistochemistry; MMP, matrix metalloproteinase; p- , phosphorylated.

Table II. Reverse transcription-quantitative PCR primer sequences.

Primer	Forward sequence (5'→3')	Reverse sequence (5'→3')
CCL3	TACAAGCAGCAGCGAGTACC	GAGCAAAGGCTGCTGGTTTC
CCL4	ACCAATGGGCTCTGACCCTC	CTTGGAGCAAAGACTGCTGGT
CCL5	CCTCACCATATGGCTCGGAC	TCTTCTCTGGGTTGGCACAC
Collagen I	GGGTTCAGCATGAGGGGATT	GGTGGAAGAGGTCAATGGGG
MMP2	CCCCATGAAGCCTTGTTTACC	GAAGGGGAAGACACATGGGG
MMP9	AAACCCTGTGTGTTCCCGTT	CGTCGCTGGTACAGGAAGAG
GAPDH	CCATCTTCCAGGAGCGAGAC	GCCCTTCCACAATGCCAAAG

CCL, C-C motif chemokine ligand; MMP, matrix metalloproteinase.

with horseradish peroxidase-conjugated secondary antibody (horseradish peroxidase-conjugated anti-rabbit immunoglobulin G; cat. no. 7074; 1:2,000; Cell Signaling Technology, Inc.), protein bands were visualized using enhanced chemiluminescence reagents (Thermo Fisher Scientific, Inc.) and quantitated by densitometric analysis using a Science Imaging system (version 4.1; Bio-Rad Laboratories, Inc.). Data were normalized to β-actin.

Histology and immunohistochemistry. The left ventricles were fixed (24 h at room temperature) in 4% paraformaldehyde, embedded in paraffin, and sliced into 4-μm sections. Tissue sections were deparaffinized in xylene, rehydrated in a descending graded alcohol series and incubated in Bouin's solution at 37˚C for 2 h. The Bouin's solution consisted of 75 ml saturated picric acid, 25 ml 10% formalin solution (v/v) and 5 ml acetic acid. Tissue sections were then stained using the Masson's Trichrome Staining kit (cat. no. G1340; Beijing Solarbio Science & Technology Co., Ltd.) according to manufacturer's protocols to assess interstitial fibrosis and collagen deposition. The collagen volume fraction (CVF; percentage of collagen-positive area) was estimated from five randomly selected visual fields of the myocardial interstitium using ImageJ imaging software (version 1.60; NIH). Collagen around blood vessels was not included in the analysis. The expression levels and distribution of CCR5 and α-smooth muscle actin (α-SMA) in myocardial tissues were examined by immunostaining using the streptavidin-biotin amplification method (22). In brief, following endogenous peroxidase inactivation (3% hydrogen peroxide; Beyotime Institute of Biotechnology) and microwave-based antigen retrieval (citric acid buffer, pH 6.0, 98˚C for a total of 30 min), sections were probed overnight at 4˚C with anti-CCR5 (1:500; cat. no. ab65850; Abcam) or anti-α-SMA antibody (1:200; cat. no. ab124964; Abcam). The staining intensity was scored as follows: 0, no staining or similar to background; 1, light staining or slightly higher than background; 2, moderate staining or significantly higher than background; 3, strong staining; and 4 very strong staining. The sections were then washed thoroughly in PBS three times for 5 min each, stained in hematoxylin for 20 sec at room temperature, dehydrated in an ascending absolute alcohol gradient, washed with xylene and mounted in synthetic resin and ImageJ software was used to assess cross-sectional areas of ventricular cardiomyocytes and inflammatory cell infiltration. All scoring was performed separately by two of the authors (WD and YL).

Cell culture and surface area determination. H9c2 cells were obtained from the American Type Culture Collection and cultured in DMEM (cat. no. C11885500BT; Invitrogen; Thermo Fisher Scientific, Inc.) supplemented with 10% FBS (cat. no. TBD31HB; Tian Jin Hao Yang Biological Manufacture Co., Ltd.) and penicillin-streptomycin (100 IU/ml) in a humidified incubator at 5% CO_2 and 37˚C. The cells were pre-incubated (37˚C for 30 min) with anti-CCR5 antibody (0.4 μg/ml; cat. no. ab65850; Abcam), isotype IgG control antibody (0.4 μg/ml; cat. no. ab190475; Abcam), according to supplier instructions, MEK inhibitor U0126 (1 μM; Sigma-Aldrich; Merck KGaA) or P38 inhibitor SB203580 (1 μM; Sigma-Aldrich; Merck KGaA) for 1 h prior to stimulation with angiotensin II (Ang II; 1 μM; Sigma-Aldrich; Merck KGaA) for 24 h at 37˚C. Cell surface area was determined using the F-actin staining method as previously described (23). In brief, according to supplier instructions, cells were washed with PBS twice and fixed in 4% paraformaldehyde for 10 min at 37˚C followed by incubation with 0.1% Triton X-100 for 20 min at 37˚C. After blocking with 5% BSA (9048-46-8; Sigma-Aldrich; Merck KGaA) for 30 min at 37˚C, the cells were incubated with Actin-Tracker Green (Beyotime Institute of Biotechnology) for 45 min at room temperature and subjected to examination by confocal laser microscopy (magnification, x100; Zeiss LSM 510 META; Zeiss AG, Oberkochen). Nuclei were counterstained with DAPI (90%; Sigma-Aldrich; Merck KGaA) at room temperature for 10 min. Images were processed using Image-Pro Plus 6.0 (Media Cybernetics, Inc.).

Statistical analysis. All data are presented as the mean ± SEM. Each experiment was repeated three times. Data were analyzed with SPSS (version 22.0; IBM Corp.) or GraphPad Prism (version 5.0; GraphPad Software, Inc.). One-way analysis of variance followed by Tukey's post hoc test was applied to determine the statistical significance of differences among groups. $P<0.05$ was considered to indicate a statistically significant difference.

Results

LV pressure overload upregulates CCR5 and its ligands in mice. Expression levels of CCR5 and its ligands (CCL3, CCL4 and CCL5) were determined in the TAC mouse model. C57BL/6 mice were subjected to TAC or sham surgery. The hearts were collected at specific time-points up to 28 days after surgery for analysis. RT-qPCR data showed time-dependent increases in myocardial CCL3, CCL4 and CCL5 mRNA expression levels, which peaked at 1-2 weeks after surgery (Fig. 1A-C). The chemokine levels then declined with time. In addition, myocardial CCR5 protein levels increased with time and peaked 2 weeks after surgery, as indicated by western blotting (Fig. 1D). CCR5 levels subsequently decreased (Fig. 1D).

CCR5 inhibition ameliorates pressure overload-induced myocardial hypertrophy and cardiac dysfunction. The effects of CCR5 inhibition on pressure overload-induced myocardial hypertrophy and cardiac dysfunction were investigated in TAC mice. ANP and BNP are two known biomarkers of cardiac hypertrophy (24). Inhibiting myocardial CCR5 decreased myocardial hypertrophy, whereas overexpression of myocardial CCR5 increased myocardial hypertrophy in the TAC heart (Fig. 2A and B). At 28 days post-surgery, immunohistochemical staining for CCR5 revealed increased myocardial CCR5 immunoreactivity in TAC hearts (Fig. 2C). The increase in myocardial CCR5 expression levels in response to TAC was accompanied by visible leukocyte infiltration and cardiomyocyte hypertrophy, as indicated by H&E staining (Fig. 2D). These histopathological changes in the pressure-overloaded hearts were associated with altered chamber dimension and impaired LV function. At 14 days post-surgery, the TAC hearts displayed decreased FS, EF and + and -dP/dt, along with increased LVEDD and LVESD (Fig. 2E-J). Compared with IgG control, anti-CCR5 antibody-treated TAC hearts

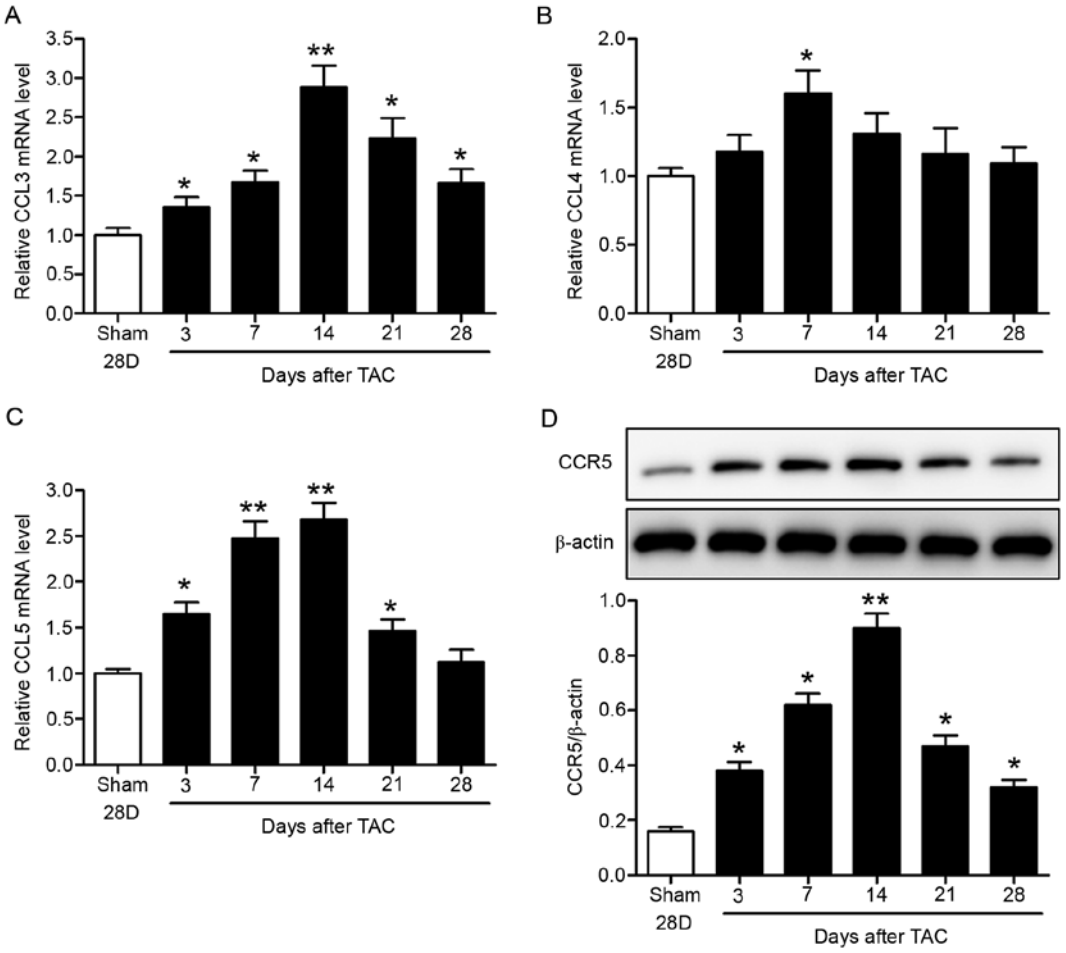

Figure 1. Pressure overload upregulates CCR5 and its ligands in mice. C57BL/6 mice were subjected to TAC or sham surgery. Myocardial tissue was collected at specific time-points up to 28 days post-surgery. Relative myocardial mRNA expression levels of (A) CCL3, (B) CCL4 and (C) CCL5 were assessed by reverse transcription-quantitative PCR. (D) Myocardial CCR5 protein expression levels were assessed by western blot analysis. TAC, n=8/time-point; Sham 28D, n=5. *P<0.05, **P<0.01 vs. Sham 28D. CCR, C-C chemokine receptor 5; TAC, transverse aortic constriction; CCL, C-C motif chemokine ligand.

exhibited decreased CCR5 immunoreactivity, leukocyte infiltration and cardiomyocyte hypertrophy and less severe cardiac dysfunction (Fig. 2A-J).

CCR5 inhibition decreases pressure overload-induced myocardial fibrosis. Myocardial fibrosis mediated by trans-differentiation of fibroblasts into myofibroblasts is a pathological response to cardiac insult such as pressure overload (25). Immunohistochemical staining revealed higher myocardial expression levels of the myofibroblast marker α-SMA in the TAC heart, compared with sham (Fig. 3A). Collagen I, MMP2 and MMP9 are known contributing factors of cardiac fibrosis and remodeling in heart disease (26). Masson's trichrome staining of LV sections showed greater collagen deposition in TAC hearts compared with sham (Fig. 3B). In addition, RT-qPCR assay revealed higher myocardial mRNA expression levels of collagen I, MMP2 and MMP9 in the TAC heart compared with sham hearts (Fig. 3C-E). Compared with IgG control, the anti-CCR5 antibody-treated TAC hearts exhibited significantly decreased myocardial α-SMA immunoreactivity and collagen deposition, as well as lower mRNA expression levels of collagen I, MMP2 and MMP9 (Fig. 3A-E). These results supported the role of CCR5 as a contributing factor in pressure overload-induced cardiac fibrosis.

CCR5 inhibition ameliorates pressure overload-induced cardiac abnormality via MAPK signaling. ERK1/2 and P38 MAPKs are considered to be central regulators of cardiac hypertrophy (27). Studies have shown that MAPK signaling induces myocardial diastolic dysfunction (28) and that activated p38 MAPK induces CCR5 to cause damage to the cell morphology and increases the percentage of cell death in rat cardiomyocytes (29). Therefore, studying the CCR5-MAPK pathway is necessary to improve understanding of cardiovascular physiology. In order to investigate the signaling mechanisms involved in the cardioprotective effects of CCR5 inhibition, myocardial ERK1/2 and P38 phosphorylation were assessed by western blot analysis. The data revealed significantly higher myocardial protein expression levels of p-ERK1/2 and p-P38 in the TAC heart compared with sham hearts 28 days after surgery (Fig. 4A). Administration of anti-CCR5 (but not IgG control antibody) inhibited ERK1/2 and P38 phosphorylation induced by TAC (Fig. 4A). In order to elucidate the molecular mechanisms involved, the effect of CCR5 inhibition on Ang II-induced hypertrophy of cultured H9c2 cardiomyocytes was investigated. Ang II significantly increased p-ERK1/2 and p-P38 levels in H9c2 cells and induced cell hypertrophy, as indicated by F-actin staining (Fig. 4B and C). Blockade of ERK1/2 by the MEK inhibitor U0126 or P38 by the P38 inhibitor SB203580 effectively attenuated cell hypertrophy

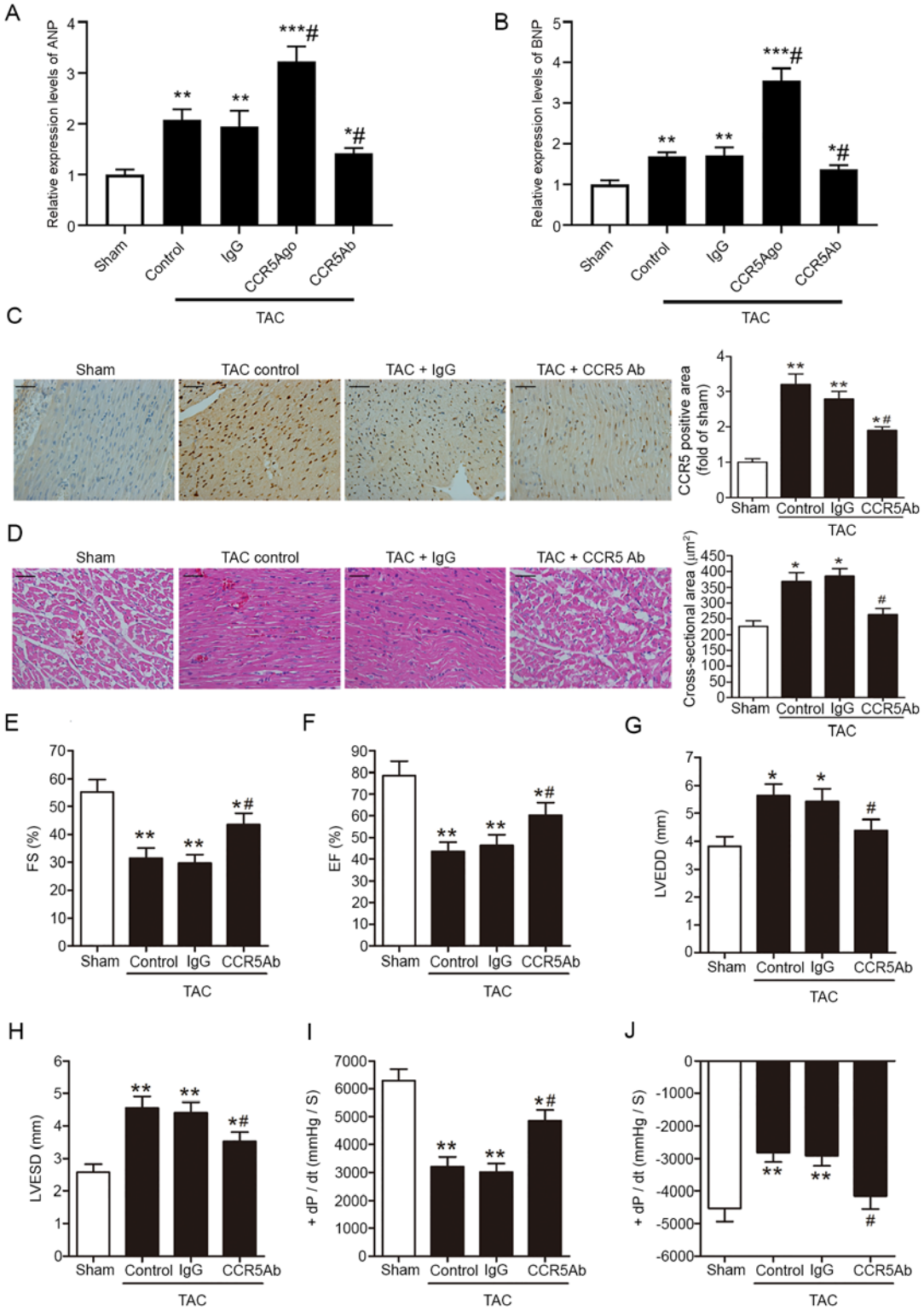

Figure 2. CCR5 inhibition ameliorates pressure overload-induced myocardial hypertrophy and cardiac dysfunction. TAC or sham mice were treated with anti-CCR5 or IgG control antibody. Relative (A) ANP and (B) BNP mRNA levels were assessed by reverse transcription-quantitative PCR. (C) Myocardial CCR5 expression levels were assessed at 28 days after surgery by immunohistochemical staining. Scale bar, 50 μm. (D) Myocardial hypertrophy (indicated in cross-sectional areas of ventricular cardiomyocytes) and inflammatory cell infiltration 28 days after surgery were assessed by hematoxylin and eosin staining. Scale bar, 50 μm. Cardiac parameters were assessed 14 days after surgery by echocardiographic and hemodynamic measurements. (E) FS, (F) EF, (G) LVEDD, (H) LVESD, (I) +dP/dt and (J) -dP/dt are shown. TAC, n=8/group; Sham, n=5. *P<0.05, **P<0.01 and ***P<0.001 vs. Sham; $^{\#}$P<0.05 vs. TAC/IgG. C-C chemokine receptor 5; TAC, transverse aortic constriction; ANP, atrial natriuretic peptide; BNP, brain natriuretic peptide; FS, fractional shortening; EF, ejection fraction; LVEDD, left ventricular end-diastolic dimension; LVESD, left ventricular end-systolic dimension; +dP/dt, maximal rate of rise in left ventricle pressure; -dP/dt, maximal rate of fall in left ventricle pressure; Ago, agonist; Ab, antibody.

induced by Ang II (Fig. 4B and C). Moreover, pre-treatment with anti-CCR5, but not IgG control antibody, inhibited ERK1/2 and P38 phosphorylation as well as cell hypertrophy induced by Ang II (Fig. 4B and C).

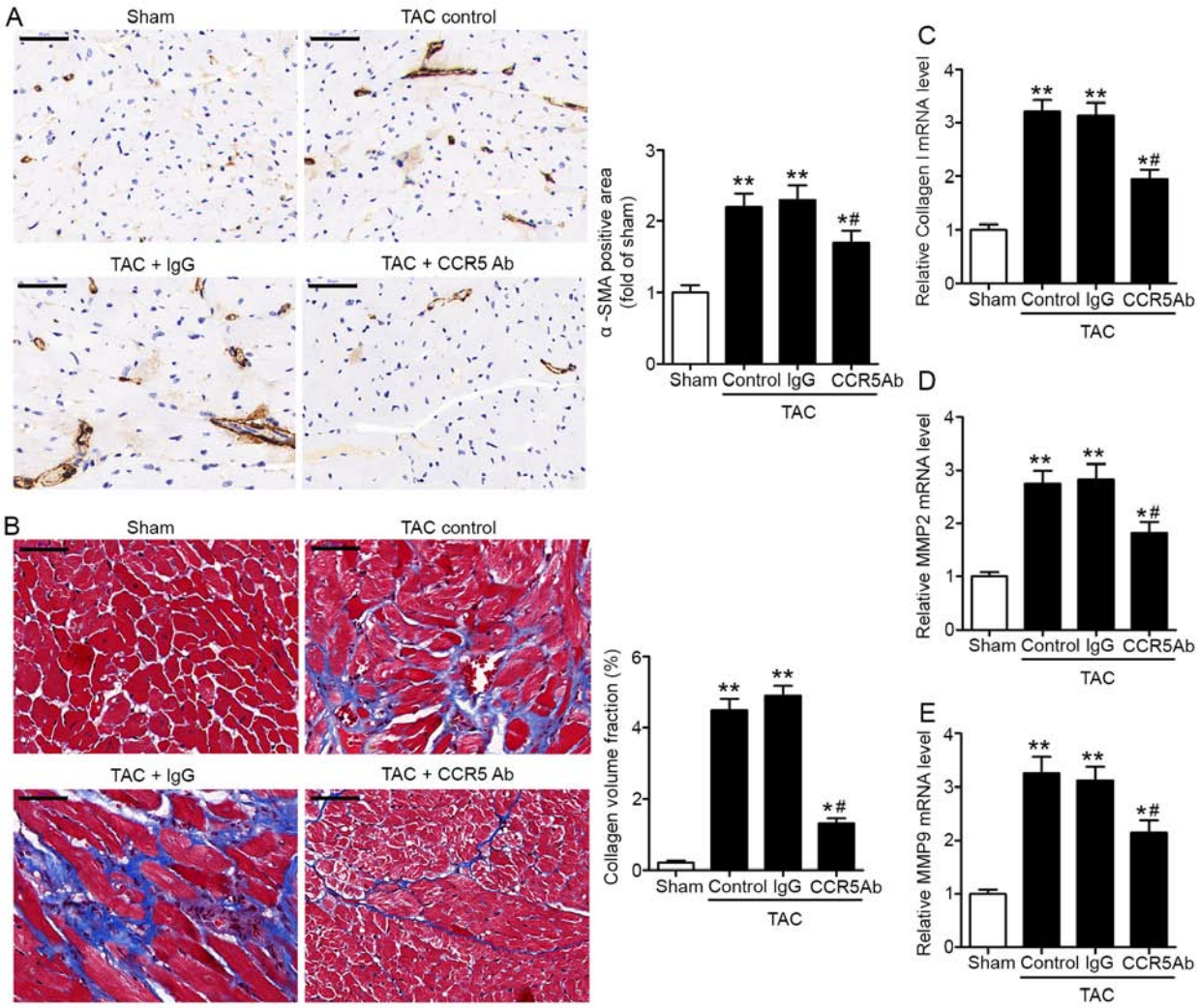

Figure 3. CCR5 inhibition decreases pressure overload-induced myocardial fibrosis. TAC or sham mice were treated with anti-CCR5 or IgG control antibody. Myocardial tissues were collected 28 days after surgery for analysis. (A) Detection of myocardial α-SMA by immunohistochemical staining. Scale bar, 50 μm. (B) Detection of left ventricle collagen deposition by Masson's trichrome staining. Scale bar, 50 μm. Collagen volume fraction was defined as the percentage of collagen-positive area. The mRNA expression levels of (C) collagen I, (D) MMP2 and (E) MMP9 in myocardial tissue were detected by reverse transcription-quantitative PCR. TAC, n=8/group; Sham, n=5. *P<0.05, **P<0.01 vs. Sham; $^{\#}$P<0.05 vs. TAC + IgG. CCR5, C-C chemokine receptor 5; TAC, transverse aortic constriction; α-SMA, α-smooth muscle actin; MMP, matrix metalloproteinase; Ab, antibody.

Discussion

CCR5 is predominantly expressed on natural killer and dendritic cells, T lymphocytes and macrophages (14). CCR5 serves a key role in human immunodeficiency virus (HIV)-1 entry into target cells, and CCR5-targeted pharmaceutical and gene therapies have been developed for clinical use against HIV (30). Research has shown that CCR5 and its ligands serve a role in autoimmune and inflammatory disease via regulation of immune cell activation and migration (14). For example, $CCR5^{+}$ inflammatory cells and increased CCR5 ligands (CCL3, CCL4 and CCL5) are found within multiple sclerosis lesions and may contribute to recruitment of inflammatory cells to the inflamed tissue and their activation (31,32). In patients with rheumatoid arthritis, $CCR5^{+}$ mononuclear cells and increased expression levels of CCR5 ligands CCL3, CCL4 and CCL5 are found in the inflamed synovium (33,34), and a non-functional CCR5 variant (CCR5 d32) is considered to exhibit a protective effect (35). Moreover, CCL5 expression levels are increased in inflammatory bowel disease (36), and CCR5 inhibition by genetic ablation or by pharmacological inhibition ameliorates both acute and chronic colitis in mice (37). CCR5 has also been implicated in development of multiple types of cancer, such as breast, prostate and colon cancer, as well as melanoma and Hodgkin lymphoma (38). The pro-tumorigenic function of CCR5 is primarily mediated by it ligand CCL5, which promotes proliferation of CCR5-positive tumor cells, recruits immunosuppressive T-regulatory cells and favors metastasis (39). Hence, the CCL5/CCR5 axis has become a potential target for development of novel anticancer therapy (40,41).

Arthrosclerosis is increasingly recognized to be a chronic inflammatory disease that involves leukocytes, such as monocytes/macrophages and T cells (42). Studies have indicated a role of CCR5 in the initiation and progression of arthrosclerosis and associated cardiovascular disease (43,44). Specifically, the CCR5 polymorphism CCR5 d32 has been linked to decreased risk of cardiovascular disease (45), and antagonism of either CCR5 or CCL5 decreases atherosclerosis in animal models (43). Additionally, CCR5 is implicated in

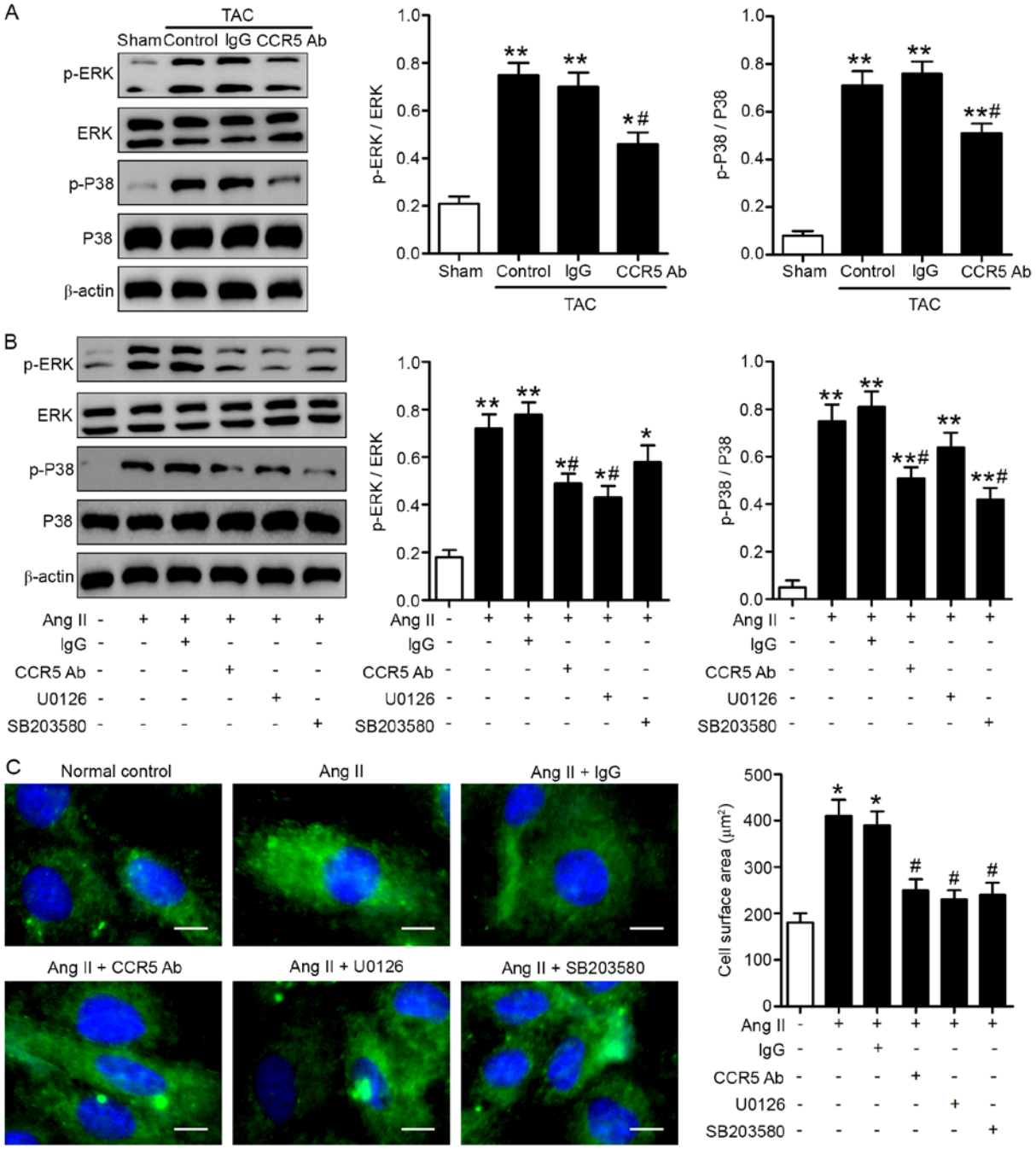

Figure 4. ERK and P38 signaling pathways are involved in the cardioprotective effects of CCR5 inhibition. (A) TAC or sham mice were treated with anti-CCR5 or IgG control antibody. Myocardial tissues were collected 28 days after surgery. Protein expression levels of p-ERK, ERK, p-P38 and P38 were determined by western blot analysis. TAC, n=8/group; Sham, n=5. *P<0.05, **P<0.01 vs. Sham; $^{\#}$P<0.05 vs. TAC + IgG. H9c2 cardiomyocytes were stimulated with Ang II for 24 h in the presence or absence of 1 h pretreatment with anti-CCR5 antibody, U0126 or SB203580. (B) p-ERK, ERK, p-P38 and P38 levels and (C) cell surface areas were determined by western blot analysis and F-actin immunofluorescence, respectively. Scale bar, 20 μm. n=3. *P<0.05, **P<0.01 vs. normal control; $^{\#}$P<0.05 vs. Ang II alone. CCR5, C-C chemokine receptor 5; TAC, transverse aortic constriction; p-, phosphorylated; Ang II, angiotensin II, Ab, antibody.

Ang II-induced hypertension and vascular dysfunction (46). Based on these previous findings, it was speculated that CCR5 may be involved in the pathogenesis of AS, a heart disease characterized by pressure overload-induced LV remodeling and dysfunction.

The present study investigated the role of CCR5 in the pathophysiology of pressure overload-induced cardiac remodeling and dysfunction in a TAC mouse model. Higher myocardial CCL3, CCL4, CCL5 and CCR5 expression levels were detected in the TAC heart compared with sham mice. Echocardiographic and hemodynamic measurements revealed cardiac abnormality in TAC mice, characterized by decreased FS, EF and maximal rates of rise and fall in LV pressure, along with LV hypertrophy. Histological examination of TAC hearts showed evidence of inflammatory cell infiltration as well as myocardial hypertrophy and fibrosis. TAC-induced LV remodeling and dysfunction were effectively ameliorated by administration of anti-CCR5 antibody, supporting CCR5 as a key factor in pressure overload-induced cardiac abnormality. Thus, pharmacological blockade of CCR5 signaling may delay

the progression of cardiac remodeling in patients with AS before valve replacement surgery.

Mechanistically, increased ERK1/2 and P38 phosphorylation was detected in TAC mice but not in sham mice in the present study, consistent with previous findings that ERK1/2 and P38 MAPKs are key regulators of cardiac hypertrophy (47,48). In the present study CCR5 inhibition attenuated myocardial ERK1/2 and P38 phosphorylation induced by TAC. By contrast, there are reports that the ERK pathway promotes compensatory hypertrophy, enhances contractile function, decreases fibrosis, and protects the heart (49,50). Studies have shown that in drug-induced liver injury, CCR5 activates M1 polarization and prevents M2 polarization via the MAPK pathway (51,52). Another study demonstrated that CCR5 silencing inhibits the inflammatory response in rheumatoid arthritis rats by inhibiting the MAPK pathway, and also inhibits viability and promotes synoviocyte apoptosis (53). Ang II has been shown to promote cardiac tissue growth and contribute to pressure overload-induced cardiac hypertrophy (54,55). In the present study, in cultured H9c2 cardiomyocytes, CCR5 inhibition decreased Ang II-induced ERK1/2 and P38 phosphorylation and cell hypertrophy. Taken together, the findings of the present study suggested that the ERK1/2 and P38 MAPK pathways were involved in the cardioprotective effects of CCR5 inhibition.

Acknowledgements

Not applicable.

Funding

The present study was supported by The National Natural Science Foundation of China (grant nos. 81760077 and 81860447), Natural Science Foundation of Inner Mongolia Autonomous Region, China (grant nos. 2018MS08053), The National Key Research and Development Program of China (grant no. 2016YFC1102502), Science and Technology Project Fund of Baotou (grant nos. 2018C2007-2-7 and 2018C2007-2-8) and Science Program Fund of Inner Mongolia Health Commission (grant no. 201703181).

Availability of data and materials

All data generated or analyzed during this study are included in this published article.

Authors' contributions

XW, WL, RZ and JH designed the entire experimental study, XW, QY and JH conducted TAC modeling, WL and RZ conducted echocardiographic and hemodynamic measurements, FL and LY conducted PCR and western blotting, WD and YL performed histology and immunohistochemistry, LX and LY performed cell culture and surface area determination, QY and WD performed data analysis, XW, RZ and JH wrote the manuscript and RZ and JH made important revisions to the manuscript and approved the published version. All authors read and approved the final manuscript.

Ethics approval and consent to participate

The study was approved by the institutional review committee of the Baotou Central Hospital in accordance with the ethical standards formulated in the Declaration of Helsinki. Standard animal care and laboratory guidelines were followed according to the IACUC protocol.

Patient consent for publication

Not applicable.

Competing interests

The authors declare that they have no competing interests.

References

1. Nkomo VT, Gardin JM, Skelton TN, Gottdiener JS, Scott CG and Enriquez-Sarano M: Burden of valvular heart diseases: A population-based study. Lancet 368: 1005-1011, 2006.
2. Rassi AN, Pibarot P and Elmariah S: Left ventricular remodelling in aortic stenosis. Can J Cardiol 30: 1004-1011, 2014.
3. Badiani S, van Zalen J, Treibel TA, Bhattacharyya S, Moon JC and Lloyd G: Aortic stenosis, a left ventricular disease: Insights from advanced imaging. Curr Cardiol Rep 18: 80, 2016.
4. Carabello BA: Aortic stenosis: From pressure overload to heart failure. Heart Fail Clin 2: 435-442, 2006.
5. Pellikka PA, Sarano ME, Nishimura RA, Malouf JF, Bailey KR, Scott CG, Barnes ME and Tajik AJ: Outcome of 622 adults with asymptomatic, hemodynamically significant aortic stenosis during prolonged follow-up. Circulation 111: 3290-3295, 2005.
6. Grimard BH and Larson JM: Aortic stenosis: Diagnosis and treatment. Am Fam Physician 78: 717-724, 2008.
7. Yarbrough WM, Mukherjee R, Ikonomidis JS, Zile MR and Spinale FG: Myocardial remodeling with aortic stenosis and after aortic valve replacement: Mechanisms and future prognostic implications. J Thorac Cardiovasc Surg 143: 656-664, 2012.
8. Gregersen I, Holm S, Dahl TB, Halvorsen B and Aukrust P: A focus on inflammation as a major risk factor for atherosclerotic cardiovascular diseases. Expert Rev Cardiovasc Ther 14: 391-403, 2016.
9. Koenen RR and Weber C: Manipulating the chemokine system: Therapeutic perspectives for atherosclerosis. Curr Opin Investig Drugs 11: 265-272, 2010.
10. Carità P, Coppola G, Novo G, Caccamo G, Guglielmo M, Balasus F, Novo S, Castrovinci S, Moscarelli M, Fattouch K, *et al*: Aortic stenosis: Insights on pathogenesis and clinical implications. J Geriatr Cardiol 13: 489-498, 2016.
11. Shioi T, Matsumori A, Kihara Y, Inoko M, Ono K, Iwanaga Y, Yamada T, Iwasaki A, Matsushima K and Sasayama S: Increased expression of interleukin-1 beta and monocyte chemotactic and activating factor/monocyte chemoattractant protein-1 in the hypertrophied and failing heart with pressure overload. Circ Res 81: 664-671, 1997.
12. Yin X, Gao Y, Shi HS, Song L, Wang JC, Shao J, Geng XH, Xue G, Li JL and Hou YN: Overexpression of SIRT6 in the hippocampal CA1 impairs the formation of long-term contextual fear memory. Sci Rep 6: 18982, 2016.
13. Finsen AV, Ueland T, Sjaastad I, Ranheim T, Ahmed MS, Dahl CP, Askevold ET, Aakhus S, Husberg C, Fiane AE, *et al*: The homeostatic chemokine CCL21 predicts mortality in aortic stenosis patients and modulates left ventricular remodeling. PLoS One 9: e112172, 2014.
14. Turner J, Steinmetz O, Stahl R and Panzer U: Targeting of Th1-associated chemokine receptors CXCR3 and CCR5 as therapeutic strategy for inflammatory diseases. Mini Rev Med Chem 7: 1089-1096, 2007.
15. Ortlepp JR, Schmitz F, Mevissen V, Weiss S, Huster J, Dronskowski R, Langebartels G, Autschbach R, Zerres K, Weber C, *et al*: The amount of calcium-deficient hexagonal hydroxyapatite in aortic valves is influenced by gender and associated with genetic polymorphisms in patients with severe calcific aortic stenosis. Eur Heart J 25: 514-522, 2004.

16. Rockman HA, Ross RS, Harris AN, Knowlton KU, Steinhelper ME, Field LJ, Ross J Jr and Chien KR: Segregation of atrial-specific and inducible expression of an atrial natriuretic factor transgene in an in vivo murine model of cardiac hypertrophy. Proc Natl Acad Sci USA 88: 8277-8281, 1991.
17. Balasubramanian S, Pleasant DL, Kasiganesan H, Quinones L, Zhang Y, Sundararaj KP, Roche S, O'Connor R, Bradshaw AD and Kuppuswamy D: Dasatinib attenuates pressure overload induced cardiac fibrosis in a murine transverse aortic constriction model. PLoS One 10: e0140273, 2015.
18. Henry WL, DeMaria A, Gramiak R, King DL, Kisslo JA, Popp RL, Sahn DJ, Schiller NB, Tajik A, Teichholz LE, *et al*: Report of the American Society of Echocardiography Committee on nomenclature and standards in two-dimensional echocardiography. Circulation 62: 212-217, 1980.
19. Ünlüer EE, Karagöz A, Bayata S and Akoğlu H: An alternative approach to the bedside assessment of left ventricular systolic function in the emergency department: Displacement of the aortic root. Acad Emerg Med 20: 367-373, 2013.
20. Toldo S, Bogaard HJ, Van Tassell BW, Mezzaroma E, Seropian IM, Robati R, Salloum FN, Voelkel NF and Abbate A: Right ventricular dysfunction following acute myocardial infarction in the absence of pulmonary hypertension in the mouse. PLoS One 6: e18102, 2011.
21. Livak KJ and Schmittgen TD: Analysis of relative gene expression data using real-time quantitative PCR and the 2(-Delta Delta C(T)) method. Methods 25: 402-408, 2001.
22. Vachon CM, Sasano H, Ghosh K, Brandt KR, Watson DA, Reynolds C, Lingle WL, Goss PE, Li R, Aiyar SE, *et al*: Aromatase immunoreactivity is increased in mammographically dense regions of the breast. Breast Cancer Res Treat 125: 243-252, 2011.
23. Wang K, Long B, Zhou J and Li PF: miR-9 and NFATc3 regulate myocardin in cardiac hypertrophy. J Biol Chem 285: 11903-11912, 2010.
24. Li X, Lan Y, Wang Y, Nie M, Lu Y and Zhao E: Telmisartan suppresses cardiac hypertrophy by inhibiting cardiomyocyte apoptosis via the NFAT/ANP/BNP signaling pathway. Mol Med Rep 15: 2574-2582, 2017.
25. Chin CWL, Everett RJ, Kwiecinski J, Vesey AT, Yeung E, Esson G, Jenkins W, Koo M, Mirsadraee S, White AC, *et al*: Myocardial fibrosis and cardiac decompensation in aortic stenosis. JACC Cardiovasc Imaging 10: 1320-1333, 2017.
26. Fan D, Takawale A, Lee J and Kassiri Z: Cardiac fibroblasts, fibrosis and extracellular matrix remodeling in heart disease. Fibrogenesis Tissue Repair 5: 15, 2012.
27. Heineke J and Molkentin JD: Regulation of cardiac hypertrophy by intracellular signalling pathways. Nat Rev Mol Cell Biol 7: 589-600, 2006.
28. Berzingi C, Chen F and Finkel MS: p38 MAP kinase inhibitor prevents diastolic dysfunction in rats following HIV gp120 injection in vivo. Cardiovasc Toxicol 9: 142-150, 2009.
29. Gao R, Fang Q, Zhang X, Xu Q, Ye H, Guo W, He J, Chen Y, Wang R, Wu Z, *et al*: R5 HIV-1 gp120 activates p38 MAPK to induce rat cardiomyocyte injury by the CCR5 coreceptor. Pathobiology 86: 274-284, 2019.
30. Haworth KG, Peterson CW and Kiem HP: CCR5-edited gene therapies for HIV cure: Closing the door to viral entry. Cytotherapy 19: 1325-1338, 2017.
31. Balashov KE, Rottman JB, Weiner HL and Hancock WW: CCR5(+) and CXCR3(+) T cells are increased in multiple sclerosis and their ligands MIP-1alpha and IP-10 are expressed in demyelinating brain lesions. Proc Natl Acad Sci USA 96: 6873-6878, 1999.
32. Boven LA, Montagne L, Nottet HS and De Groot CJ: Macrophage inflammatory protein-1alpha (MIP-1alpha), MIP-1beta, and RANTES mRNA semiquantification and protein expression in active demyelinating multiple sclerosis (MS) lesions. Clin Exp Immunol 122: 257-263, 2000.
33. Mack M, Brühl H, Gruber R, Jaeger C, Cihak J, Eiter V, Plachý J, Stangassinger M, Uhlig K, Schattenkirchner M, *et al*: Predominance of mononuclear cells expressing the chemokine receptor CCR5 in synovial effusions of patients with different forms of arthritis. Arthritis Rheum 42: 981-988, 1999.
34. Patel DD, Zachariah JP and Whichard LP: CXCR3 and CCR5 ligands in rheumatoid arthritis synovium. Clin Immunol 98: 39-45, 2001.
35. Pokorny V, McQueen F, Yeoman S, Merriman M, Merriman A, Harrison A, Highton J and McLean L: Evidence for negative association of the chemokine receptor CCR5 d32 polymorphism with rheumatoid arthritis. Ann Rheum Dis 64: 487-490, 2005.
36. McCormack G, Moriarty D, O'Donoghue DP, McCormick PA, Sheahan K and Baird AW: Tissue cytokine and chemokine expression in inflammatory bowel disease. Inflamm Res 50: 491-495, 2001.
37. Mencarelli A, Cipriani S, Francisci D, Santucci L, Baldelli F, Distrutti E and Fiorucci S: Highly specific blockade of CCR5 inhibits leukocyte trafficking and reduces mucosal inflammation in murine colitis. Sci Rep 6: 30802, 2016.
38. Aldinucci D and Colombatti A: The inflammatory chemokine CCL5 and cancer progression. Mediators Inflamm 2014: 292376, 2014.
39. de Oliveira CE, Oda JM, Losi Guembarovski R, de Oliveira KB, Ariza CB, Neto JS, Banin Hirata BK and Watanabe MA: CC chemokine receptor 5: The interface of host immunity and cancer. Dis Markers 2014: 126954, 2014.
40. Velasco-Velázquez M, Xolalpa W and Pestell RG: The potential to target CCL5/CCR5 in breast cancer. Expert Opin Ther Targets 18: 1265-1275, 2014.
41. Bronte V and Bria E: Interfering with CCL5/CCR5 at the tumor-stroma interface. Cancer Cell 29: 437-439, 2016.
42. Weber C, Zernecke A and Libby P: The multifaceted contributions of leukocyte subsets to atherosclerosis: Lessons from mouse models. Nat Rev Immunol 8: 802-815, 2008.
43. Jones KL, Maguire JJ and Davenport AP: Chemokine receptor CCR5: From AIDS to atherosclerosis. Br J Pharmacol 162: 1453-1469, 2011.
44. de Jager SC, Kraaijeveld AO, Grauss RW, de Jager W, Liem SS, van der Hoeven BL, Prakken BJ, Putter H, van Berkel TJ, Atsma DE, *et al*: CCL3 (MIP-1 alpha) levels are elevated during acute coronary syndromes and show strong prognostic power for future ischemic events. J Mol Cell Cardiol 45: 446-452, 2008.
45. Afzal AR, Kiechl S, Daryani YP, Weerasinghe A, Zhang Y, Reindl M, Mayr A, Weger S, Xu Q and Willeit J: Common CCR5-del32 frameshift mutation associated with serum levels of inflammatory markers and cardiovascular disease risk in the Bruneck population. Stroke 39: 1972-1978, 2008.
46. Mettimano M, Specchia ML, Ianni A, Arzani D, Ricciardi G, Savi L and Romano-Spica V: CCR5 and CCR2 gene polymorphisms in hypertensive patients. Br J Biomed Sci 60: 19-21, 2003.
47. Rose BA, Force T and Wang Y: Mitogen-activated protein kinase signaling in the heart: Angels versus demons in a heart-breaking tale. Physiol Rev 90: 1507-1546, 2010.
48. Marber MS, Rose B and Wang Y: The p38 mitogen-activated protein kinase pathway - a potential target for intervention in infarction, hypertrophy, and heart failure. J Mol Cell Cardiol 51: 485-490, 2011.
49. Mutlak M, Schlesinger-Laufer M, Haas T, Shofti R, Ballan N, Lewis YE, Zuler M, Zohar Y, Caspi LH and Kehat I: Extracellular signal-regulated kinase (ERK) activation preserves cardiac function in pressure overload induced hypertrophy. Int J Cardiol 270: 204-213, 2018.
50. Schiattarella GG: Extracellular signal-regulated kinase (ERK) in left ventricular pathological hypertrophy: Not a new kid on the block anymore. Int J Cardiol 271: 260-261, 2018.
51. Li M, Sun X, Zhao J, Xia L, Li J, Xu M, Wang B, Guo H, Yu C, Gao Y, *et al*: CCL5 deficiency promotes liver repair by improving inflammation resolution and liver regeneration through M2 macrophage polarization. Cell Mol Immunol 17: 753-764, 2020.
52. Suarez-Carmona M, Chaorentong P, Kather JN, Rothenheber R, Ahmed A, Berthel A, Heinzelmann A, Moraleda R, Valous NA, Kosaloglu Z, *et al*: CCR5 status and metastatic progression in colorectal cancer. OncoImmunology 8: e1626193, 2019.
53. Lan YY, Wang YQ and Liu Y: CCR5 silencing reduces inflammatory response, inhibits viability, and promotes apoptosis of synovial cells in rat models of rheumatoid arthritis through the MAPK signaling pathway. J Cell Physiol 234: 18748-18762, 2019.
54. Zhai P, Yamamoto M, Galeotti J, Liu J, Masurekar M, Thaisz J, Irie K, Holle E, Yu X, Kupershmidt S, *et al*: Cardiac-specific overexpression of AT1 receptor mutant lacking G alpha q/G alpha i coupling causes hypertrophy and bradycardia in transgenic mice. J Clin Invest 115: 3045-3056, 2005.
55. Yu CJ, Tang LL, Liang C, Chen X, Song SY, Ding XQ, Zhang KY, Song BL, Zhao D, Zhu XY, *et al*: Angiotensin-converting enzyme 3 (ACE3) protects against pressure overload-induced cardiac hypertrophy. J Am Heart Assoc 5: 5, 2016.